Modelling the role of HIF in the regulation of metabolic key genes LDH and PDH: Emergence of Warburg Phenotype.

Kévin SPINICCI[1,2], Pierre JACQUET[1], Gibin POWATHIL[2], and Angélique STEPHANOU[1]

[1]Univ. Grenoble Alpes, CNRS, UMR 5525, VetAgro Sup, Grenoble INP, TIMC, 38000 Grenoble, France

[2]Department of Mathematics - Swansea University

February 2022

Abstract

Oxygenation of tumours and the effect of hypoxia in cancer cell metabolism is a widely studied subject. Hypoxia Inducible Factor (HIF), the main actor in the cell response to hypoxia, represents a potential target in cancer therapy. HIF is involved in many biological processes such as cell proliferation, survival, apoptosis, angiogenesis, iron metabolism and glucose metabolism. This protein regulates the expressions of Lactate Dehydrogenase (LDH) and Pyruvate Dehydrogenase (PDH), both essential for the conversion of pyruvate to be used in aerobic and anaerobic pathways. HIF upregulates LDH, increasing the conversion of pyruvate into lactate which leads to higher secretion of lactic acid by the cell and reduced pH in the microenvironment. HIF indirectly downregulates PDH, decreasing the conversion of pyruvate into Acetyl Coenzyme A which leads to reduced usage of the Tricarboxylic Acid (TCA) cycle in aerobic pathways. Upregulation of HIF may promote the use of anaerobic pathways for energy production even in normal extracellular oxygen conditions. Higher use of glycolysis even in normal oxygen conditions is called the Warburg effect. In this paper, we focus on HIF variations during tumour growth and study, through a mathematical model, its impact on the two metabolic key genes PDH and LDH, to investigate its role in the emergence of the Warburg effect. Mathematical equations describing the enzymes regulation pathways were solved for each cell of the tumour represented in an agent-based model to best capture the spatio-temporal oxygen variations during tumour development caused by cell consumption and reduced diffusion inside the tumour. Simulation results show that reduced HIF degradation in normoxia can induce higher lactic acid production. The emergence of the Warburg effect appears after the first period of hypoxia before oxygen conditions return to a normal level. The results also show that targeting the upregulation of LDH and the downregulation of PDH could be relevant in therapy.

Introduction

Cells rely on two main processes to produce ATP: Oxidative Phosphorylation (OXPHOS) by using oxygen, and glycolysis by using glucose. Glycolysis is a pathway generating both ATP and pyruvate using glucose as input [1, 2, 3]. Pyruvate produced by glycolysis can then be used to fuel the Tricarboxylic Acid (TCA) cycle and produce the compounds involved in OXPHOS, the aerobic pathway. If oxygen is not present, pyruvate is turned into lactate, this process is called fermentation [4]. Lactate formed during fermentation is secreted into the microenvironment which causes a decrease in extracellular pH.

In 1927, Otto Warburg observed that the tumour consumed more glucose and produced more lactic acid than normal tissues [5]. At first Warburg's observation didn't consider the presence of oxygen, yet since increased lactic acid production was also observed when oxygen is available, it has slowly been associated with aerobic glycolysis [6]. Nowaday, high rate of glycolysis, even if oxygen is available, is known as the Warburg Effect [7, 8]. In this paper, we will retain this definition. Tumours can develop anywhere, yet harsh conditions favour tumour appearance [9]. Most tumours have median oxygen levels falling below 2%, the threshold at which the hypoxic response is half-maximal [10]. For this reason, a lot of interest has been put in the effect of oxygenation on tumour metabolism and specifically on the Hypoxia Inducible Factor (HIF) protein. This protein, being the main actor in the cell response to hypoxia, is interesting to explore as a potential target for cancer therapy since hypoxic cells are more radioresistant [10, 7].

HIF Structure and Mechanism of action

The HIF protein was discovered by Semenza and co-workers during a study on the erythropoietin (EPO) gene, a gene encoding for the erythropoietin hormone involved in red blood cells production, in 1991 [11]. They found DNA sequences in the gene important for its transcriptional activation in hypoxic conditions, now called Hypoxia Response Elements (HRE). The HIF protein is a heterodimer composed of two subunits HIF-1α and HIF-1β, it acts as a transcription factor by binding to HRE in hypoxic conditions. The subunit HIF-1α is oxygen-sensitive and degraded in presence of oxygen, compared to the constitutively expressed HIF-1β subunit. Three isoforms of the α subunit have been identified: HIF-1α, HIF2-α and HIF3-α. HIF-1α and HIF2-α are the most studied of the three homologs, HIF-1α is expressed ubiquitously in the body while HIF2-α expression is tissue-specific [11]. It has been demonstrated that overexpression or suppression of HIF-1α or HIF2-α influence each other *in vitro* and one homolog can be more expressed than the other. Kidney lesions with early VHL inactivation show more activation of HIF-1α than HIF-2α but this balance can change [12]. Transcriptional activity of HIF-1α requires the binding of the co-factor CBP/p300 to the C-TAD domain of HIF-1α, then HIF will bind to HRE and activate the transcription of its target genes [11, 13, 14].

HIF regulation

Oxygen-dependent regulation of HIF-1α is mainly done by Prolyl Hydroxylase (PHD) and FIH-1 enzymes. They act at the posttranslational level by inducing its degradation or disrupting its interaction

with co-factors. Prolyl Hydroxylase (PHD) proteins catalyze the hydroxylation of proline residues, targeting HIF-1α for proteasomal degradation by the Von Hippel-Lindau (VHL) tumour suppressor protein. Hydroxylation of asparagine residues by Factor Inhibiting HIF-1 (FIH-1) inhibits the interaction between HIF-1α and the important co-factor CBP/p300, preventing regulation of HIF-1α target genes. Since PHD and FIH-1 need oxygen to hydroxylate HIF-1α residues, they act as oxygen sensors in the cell response to hypoxia. Hypoxia promotes HIF-1α protein stability and transcriptional activity. Reactive Oxygen Species (ROS) and oncometabolites such as succinate, fumarate, lactate upregulate HIF-1α [14].

Oxygen-independent mechanisms regulating HIF-1α transcription and translation include PI3K/Akt/ mTOR and RAS/RAF/MEK/ERK pathways. Multiple growth factors, oncogenes, mutations (such as in the tumour suppressor genes PTEN and p53) or ROS may increase HIF-1α levels through PI3K and RAS signalling cascade [14, 11, 13]. A study by The Cancer Genome Atlas (TCGA) identified the most altered genes in glioblastoma, it reveals that RTK/RAS/PI3K are among the frequently altered pathways in this disease [15]. It suggests that HIF is a strong candidate for cancer therapy, not only because of its role in the cellular response to hypoxia but also for its frequent deregulation in cancer as well. HIF regulation is summarized in figure 1.

Impact on cellular biological functions

The cell response to hypoxia initiated by HIF affects many biological processes such as cell proliferation, survival, apoptosis, angiogenesis, iron metabolism and glucose metabolism [13]. Pathway enrichment analysis of 98 HIF target genes revealed 20 pathways including those implicated in cancer, glycolysis/gluconeogenesis and metabolism of carbohydrates [16].

HIF can prevent G1/S transition through the regulation of cyclin-dependent kinase inhibitors (p21, p27) and cyclin proteins (cyclin G2, cyclin E) [17]. Cyclin E downregulation is mediated through the inhibition of cyclin D by HIF causing a slowing down or arrest of the cell cycle in the G1 phase and promoting the entry into quiescence, which can be a mechanism to escape chemotherapy [18].

The Warburg effect is caused by an increase in glucose utilization by the cells, the glycolysis being one of the pathways affected by hypoxia. HIF increases the expression of glucose transporters GLUT1 and GLUT3 which contain HRE in their promoters, resulting in higher glucose uptake [19]. Furthermore, HIF induces the overexpression of specific glycolytic isoforms for each enzyme involved in all the steps of the glycolysis [20]. Thus, HIF upregulates the expression of Lactate Dehydrogenase (LDH), an enzyme that catalyzes the reversible reaction in which pyruvate is converted to lactate, resulting in higher lactate secretion which acidifies the microenvironment.

TCA cycle works in cooperation with the OXPHOS to produce ATP. Pyruvate produced by the last steps of the glycolysis is turned into Acetyl Coenzyme A by Pyruvate Dehydrogenase (PDH) to fuel the TCA cycle, promoting an oxidative metabolism. However, Pyruvate Dehydrogenase Kinase (PDK) an inhibitor of PDH is upregulated by HIF [21]. Not only hypoxia will increase the use of glycolysis by the cell, but it will also reduce the use of TCA cycle.

In this paper, we want to study how genetic (or epigenetic) regulations, between HIF and its two targets LDH and PDH, may affect the emergence of the Warburg effect. The Warburg effect results in
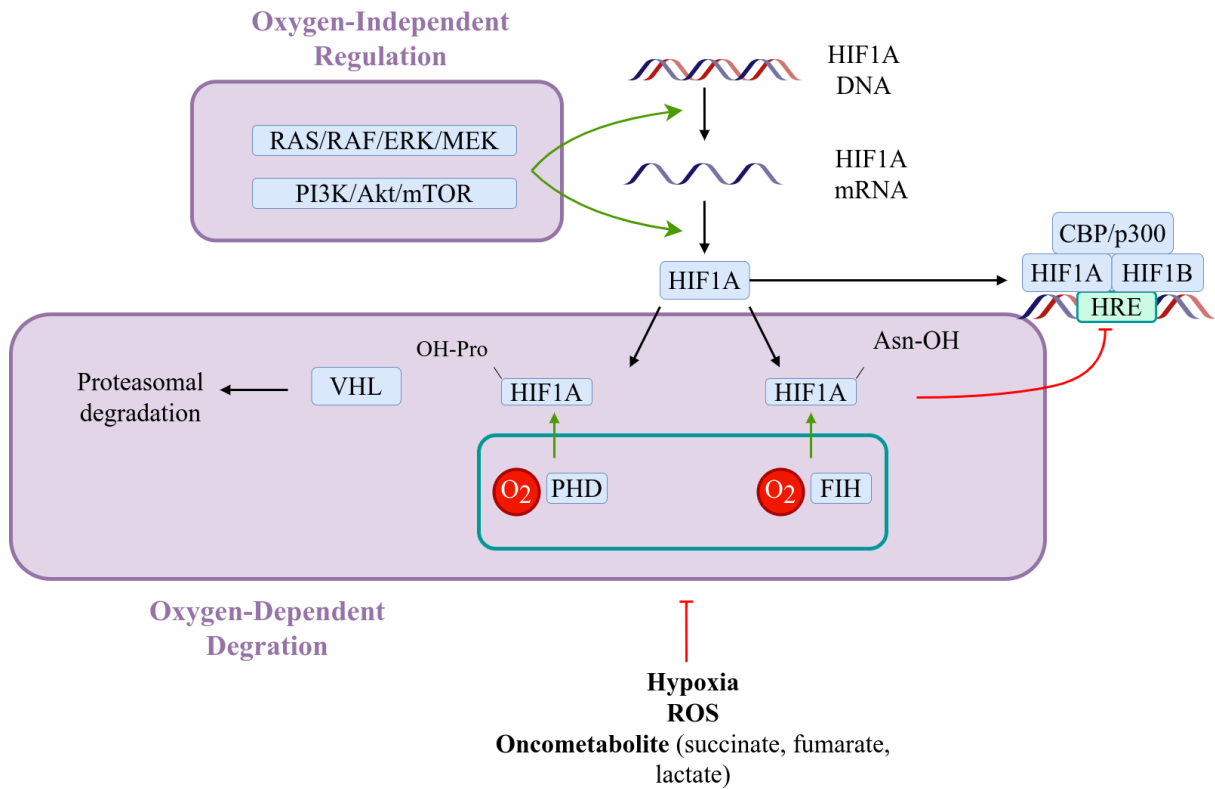
Figure 1: Regulation of Hypoxia Inducible Factor by oxygen-dependent and oxygen-independent mechanisms. PI3K/Akt/mTOR and RAS/RAF/ERK/MEK signalling pathways increase HIF transcription and translation in an oxygen-independent way. The oxygen-dependent regulation relies mainly on the two enzymes: PHD and FIH-1. PHD catalyzes the oxygen-dependent hydroxylation of proline residues on the HIF protein, which is then targeted for proteasomal degradation by the VHL. FIH-1 catalyzes the oxygen-dependent hydroxylation of asparagine residues, which inhibits the interaction between the HIF protein and the CBP/p300 co-factor. Hydroxylation of HIF residues by PHD and FIH-1 is inhibited by hypoxia, ROS and oncometabolites such as succinate, fumarate and lactate.

an increased production of lactic acid by the tumour by metabolizing glucose, even in normoxia [22, 7, 8, 23, 24].

Material and Method

Genetic Regulations

Here, we assume that HIF plays a major role in mediating the cell response to hypoxia. We have selected LDH and PDH to model the effect of hypoxia on metabolism since (1) they are key enzymes for the conversion of pyruvate into lactate/AcetylCoA respectively after the glycolysis, and (2) they are both regulated by HIF directly or indirectly. PDH is downregulated by HIF through its inhibitor PDK, therefore PDK will be included in the model (see figure 2). Genetic regulations are based on the model described by Li *et al* [21]. All genetic regulations are described by the following equations:

$$\frac{dHIF}{dt} = A_{HIF} - D_{HIF} \times H^+_{O_2 \to HIF} \times HIF \tag{1}$$

$$\frac{dLDH}{dt} = A_{LDH} \times H^+_{HIF \to LDH} - D_{LDH} \times LDH \tag{2}$$

$$\frac{dPDK}{dt} = A_{PDK} \times H^+_{HIF \to PDK} - D_{PDK} \times PDK \tag{3}$$

$$\frac{dPDH}{dt} = A_{PDH} \times H^-_{PDK \to PDH} - D_{PDH} \times PDH \tag{4}$$

where A is a parameter for gene production and D for gene degradation. LDH and PDK upregulations by HIF and PDH downregulations by PDK are described with a non-linear function named the shifted-Hill function. In the same way, the increased HIF protein degradation in normoxia is described using the same function. The shifted-Hill function has the form:

$$H^{+/-}_{Y \to Z} = \frac{S^n}{S^n + Y^n} + \gamma_{Y \to Z} \frac{Y^n}{S^n + Y^n}.$$

Here, $H_{Y \to Z}$ represents the effect of the regulating gene Y on the regulated gene Z. $H^+_{Y \to Z}$ indicates an upregulation, while $H^-_{Y \to Z}$ is a downregulation. S is the gene level with a half-threshold of production. The positive parameter γ represents an activation if > 1 or an inhibition if < 1. All genes levels are dimensionless, parameters used in the equation above are summarised in table 1.

Cell Metabolism

Cells consume glucose and oxygen to produce ATP. Nutrient consumption rates change over time depending on microenvironment conditions. In normoxia, cells mostly use aerobic pathways (glycolysis + OXPHOS) which produce more ATP per mole mole of glucose consumed than anaerobic pathways (glycolysis + lactate production). In hypoxia, the cell metabolism transits toward a glycolytic pathway involving lactate production. Cells consumption and production are derived from the model described by [25]. Here, the impact of the level of genes on metabolism is modelled by a non-linear function to tune the maximal consumption of oxygen and glucose. Furthermore, LDH and PDH levels are used to tune glycolysis and TCA pathways in the model as they have an important role in the conversion of pyruvate

Parameter	Value	Dimension	Parameter	Value	Dimension
A_{HIF}	0.05	1/min	D_{HIF}	0.005	1/min
A_{LDH}	0.005	1/min	D_{LDH}	0.005	1/min
A_{PDK}	0.005	1/min	D_{PDK}	0.005	1/min
A_{PDH}	0.005	1/min	D_{PDH}	0.005	1/min
$S_{O_2 \rightarrow HIF}$	0.02085	mmol/L	$S_{HIF \rightarrow LDH}$	4.48	-
$S_{HIF \rightarrow PDK}$	5.0	-	$S_{PDK \rightarrow PDH}$	2.2	-
$\gamma_{O_2 \rightarrow HIF}$	10.0	-	$\gamma_{HIF \rightarrow LDH}$	3.61	-
$\gamma_{HIF \rightarrow PDK}$	6.97	-	$\gamma_{PDK \rightarrow PDH}$	0.14	-

Table 1: Parameters used in genetics regulations. The absence of unit means that the parameter is dimensionless.

[26]. We define p_O and p_G, two terms to adjust the consumption rates of oxygen and glucose according to their respective key enzyme level in the form:

$$p_X = \frac{p_{X_{MAX}} - p_{X_{MIN}}}{1 + \exp\left(-l_X(X - X_0)\right)} + p_{X_{MIN}}$$

Here, $p_{X_{MAX}}$ and $p_{X_{MIN}}$ are both the maximal and minimal value of p_X. X is the current level of genes, X_0 the midpoint of the function and l_X is the steepness of the curve.

Oxygen consumption is determined using a Michaelis-Menten function [25]:

$$f_O = p_O V_O \frac{O_e}{O_e + K_O}$$

PDH allows the pyruvate to enter the TCA cycle as Acetyl Coenzyme A, it is a limiting step in the aerobic pathway. This is included in the model by adjusting the maximum oxygen consumption rate V_O using the term p_O to represent PDH level effect on metabolism. O_e is the extracellular oxygen concentration. K_O is the extracellular oxygen concentration at which the cell oxygen consumption rate is half-maximum.

Following Robertson-Tessi *et al* [25], we assume that ATP demand drives glucose consumption. In low oxygen conditions, the cell will consume more glucose to produce ATP in the last step of the glycolysis, then pyruvate is turned into lactate by the LDH enzyme. An increase of LDH indicates an upregulation of anaerobic pathways which means here, an increase in glucose consumption. We use the term p_G to describe this phenomenon in the equation [25]:

$$f_G = (\frac{p_G A_0}{2} - \frac{29 f_O}{10})\frac{G_e}{G_e + K_G}$$

A_0 is the target ATP production. G_e is the extracellular glucose concentration. K_G is the extracellular glucose concentration at which the glucose consumption rate is half-maximal.

We take the same stoichiometric coefficients as in [25]: glycolysis uses 1 mole of glucose produces 2 moles of ATP, aerobic pathway uses 1 mole of glucose and 5 moles of oxygen to produce 29 moles of ATP. We can compute the ATP produced from the nutrients consumed using the yield from glycolysis and aerobic pathway [25]:
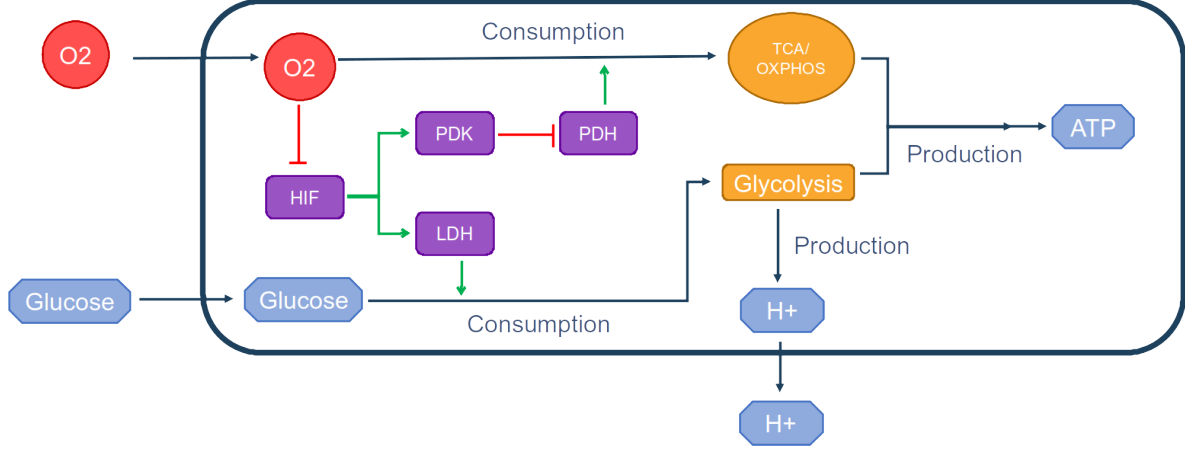
$$f_{ATP} = 2 f_G + \frac{29 f_O}{5}$$

Figure 2: Cell metabolism and genetic regulations implemented in the model. Green arrows represent upregulation, red arrows represent inhibition.

Glycolysis produces 2 moles of pyruvate with 1 mole of glucose. If oxygen is absent, pyruvate is turned into lactate, giving a total of 2 moles of lactate [4]. Lactic acid production is given by the glucose consumed:

$$f_{H^+} = k_H 2 f_G$$

k_H is a fixed parameter for proton buffering (dimensionless).

Quantities consumed and produced by one cell are modelled using the ODE:

$$\frac{dX}{dt} = f_X \tag{5}$$

with X is the molecule consumed or produced by the cell. The four variables described are oxygen (O), glucose (G), ATP (ATP), and protons (H$^+$).

The extracellular quantities of three molecules oxygen (O), glucose (G) and protons (H$^+$) are described in the model by:

$$\frac{\partial X}{\partial t} = \begin{cases} D_X \nabla^2 X - f_X^i, \text{ if X=\{O, G\}} \\ D_X \nabla^2 X + f_X^i, \text{ if X=H}^+ \end{cases} \tag{6}$$

X is the diffusible molecule, D_X is the diffusion coefficient for molecule X, f_X^i describe the impact of each cell i on the extracellular concentration.

Parameters used in those functions are summarised in table 2. The schematic in figure 2 shows the cellular metabolism and the genetics regulation implemented in the model.

Numerical Implementation

The tumour microenvironment plays a vital role in the growth and progression of tumour cells. As the tumour grows, intracellular and intercellular interactions influence the changes in its microenvironment, which can further result in cells dynamic. Here, we aim to develop a modelling framework to simulate the growth of a large population of cells cultured *in vitro*, each cell having its metabolism influenced by the

Parameter	Value	Unit
V_O	0.01875	mmol/L/min
K_O	0.0075	mmol/L
K_G	0.04	mmol/L
k_H	2.5e-4	-
A0	0.10875	mmol/L/min
pG_{MAX}	50	-
pG_{MIN}	1	-
l_G	4	-
LDH_0	2.35	-
po_{MAX}	1	-
po_{MIN}	0	-
l_O	15	-
PDH_0	0.575	-

Table 2: Parameters for metabolism. Dimensionless unit are indicated with -.

microenvironment conditions to represent accurately the resources dynamics in the tumour. Therefore, the numerical implementation of the model must have sufficient performance to simulate the behaviour of thousands of cells. In this regard, we selected Physicell, an open-source C++ framework designed to run simulations containing a large population of cells. This framework has good performance with a low memory footprint, allows the user to implement his custom code and define custom cell types, run a multi-agent-based simulation in 2D or 3D [27].

Here, the impact of extracellular oxygen concentration is studied considering different boundary conditions: physiological normoxia at 0.056 mmol/L (5% O_2), pathological hypoxia at 0.01112 mmol/L (1% O_2) and a last where boundary conditions are modified during the simulation from physiological normoxia to pathological hypoxia. The hypoxia threshold is set at 0.02085 (2% O_2), the level at which HIF has a half-maximal response [10].

The governing ODEs (equation 1 - 5) and PDEs (equation 6) are run at each timestep to compute cell nutrient consumption, energy and acidity production for that period. After each time step, the cell state is updated according to the quantity of ATP generated and the extracellular pH. Therefore, cells can proliferate and divide only if they were able to generate enough ATP and if extracellular pH is higher than the acid resistance of the cell (6.1 [25]). If the quantity of ATP generated is less than a threshold $ATP_{quiescence}$, the cell enters quiescence and is then prevented to complete the G1 phase. If the quantity of ATP generated is less than a threshold ATP_{death} or if the pH is less than a threshold pH_{death}, the cell dies and enters into the death cycle where it is progressively removed from the microenvironment by lysis. Cell cycle phase transition is handled by the PhysiCell software. Phases duration are 5h in G1, 8h in S, 4h in G2 and 1h in M, for a total of 18h to complete a cell cycle [28].

Results

Qualitative exploration of the model at the cell scale

A well-known phenomenon is the Warburg effect, increased production of lactic acid by the tumour [5] even in normoxia [22, 7, 8]. A qualitative study of the genetic deregulations at the cell scale would reveal how it impacts lactic-acid production to investigate the appearance of the Warburg effect. The primary aim of this study is to investigate the role of genetic regulations in cell metabolic changes.

In our mathematical model, the regulating effect of a gene on another is mainly driven by the γ parameter in the shifted-Hill function. Setting this parameter equal to 1 simulate a loss of the regulating function. An over-sensitivity of a gene by its regulator is modelled by setting the γ parameter to 40, the maximum defined in the model from [21]. Results of a few regulations are shown in figure 3.

When no genetic deregulations are applied to the model (figure 3.A), protons production range from 0.0001 mmol/L/min to 0.001 mmol/L/min with normal γ parameters. Around 0.01 mmol/L oxygen (1%), the cell progressively increases its H^+secretion rate from 0.0001 mmol/L/min to the maximum 0.001 mmol/L/min.

In our model, when HIF is not subjected to oxygen degradation (figure 3.B), the rate of H^+production is only influenced by glucose concentration. In this case, cell's lactic-acid secretion rate can reach 0.001 mmol/L/min even in normal oxygen pressure, as a result of the Warburg effect. Increased degradation of HIF in oxygen (figure 3.C) reduces the oxygen threshold at which the cell has a lactic-acid secretion rate of 0.001 mmol/L/min. Lower levels of oxygen are needed to reach the maximal secretion rate compared to the normal degradation rate of HIF. With no deregulation (figure 3.A), the lactic-acid secretion rate starts to increase at around 0.019 mmol/L of oxygen and reach a maximum at around 0.08 mmol/L. With increased HIF degradation by oxygen (figure 3.C), this span is reduced and lactic-acid secretion increases at around 0.012 mmol/L of oxygen. Similar to our result, a model from [23] shows that a lower degradation rate of HIF increases the chance that cells use glycolysis instead of OXPHOS, which will increase lactic acid secretions.

Inhibiting LDH sensitivity to HIF (figure 3.D) causes the maximum lactic-acid secretion rate to fall to 0.0008 mmol/L/min. Increasing LDH sensitivity to HIF does not permit the cell to have a higher H^+production rate in normoxia, while a decrease prevents a high H^+production rate in hypoxia (results not shown).

Interfering with PDK sensitivity to HIF or PDH sensitivity to PDK seems to have no effect on acid production in the model but on oxygen consumption by the cell (results not shown).
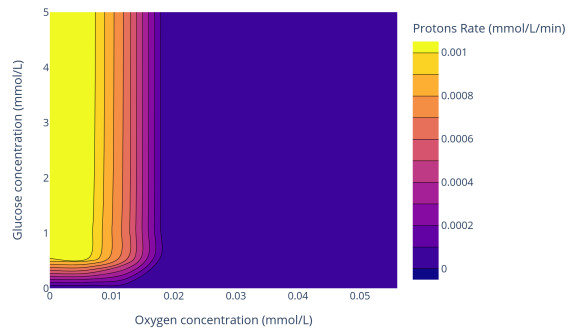
Exploration of environment and genetic properties on the emergence of the Warburg phenotype

Influence of environmental oxygen conditions

The Warburg effect is currently defined as high production of acidity due to the use of glycolysis even in normoxia [23, 24, 9]. We ran several simulations with different environmental oxygen conditions to assess
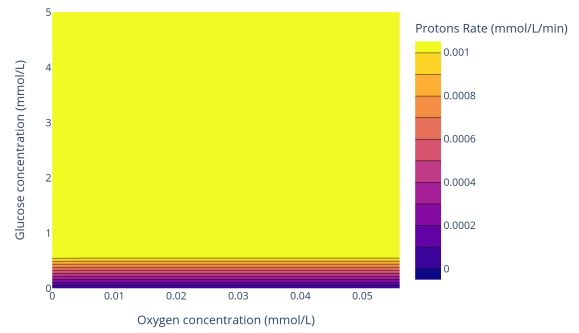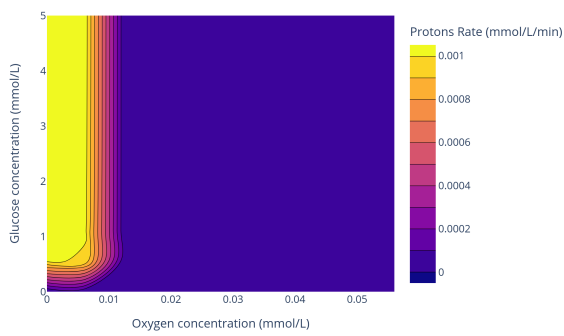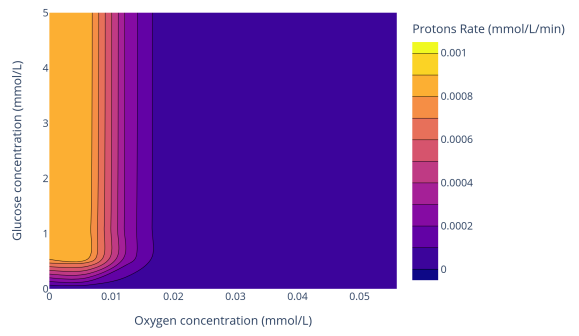
Figure 3: Influence of genetic upregulation or inhibition on the production rate of protons at different glucose and oxygen concentrations. (A) Result with no genetic deregulation. (B) Result with inhibition of the oxygen-dependant degradation of HIF. (C) Result with over-degradation of HIF by oxygen. (D) Result with loss of upregulation of LDH by HIF.
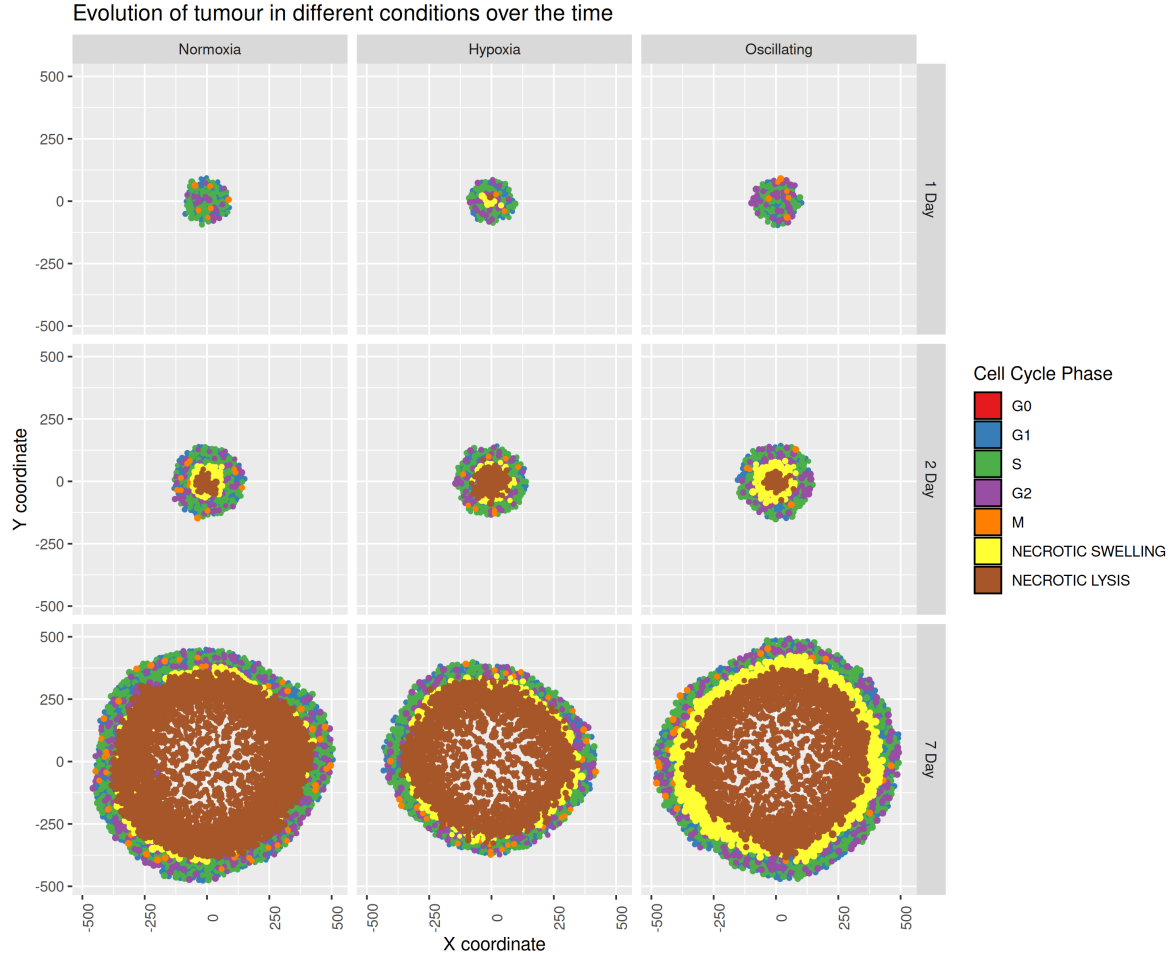
Figure 4: Evolution of tumour growth at different times in different conditions. In oscillating conditions, the oxygen concentration is slowly decreased from normoxia to hypoxia during 6 hours, then cells are slowly put back in normoxia at the same rate. This process is repeated until the end of the simulation.

whether microenvironmental conditions only, can induce a Warburg effect in the model.

Figure 4 shows how oxygen conditions affect tumour growth. In oscillating conditions, the oxygen concentration varies between physiological normoxia and pathological hypoxia and reverse every 6 hours until the end of the simulation. Kinetics of HIF show a peak after 6h and a decrease to an equilibrium state after 24h-48h. We choose to simulate 6h-period of hypoxia/normoxia to avoid the cell reaching an equilibrium and to simulate stressful conditions with a high response to a low level of oxygen. Constant hypoxia slows down tumour growth and reduces tumour diameter compared to normoxia. In all 3 different conditions, the centre of the tumour is composed of dead cells surrounded by living cells at the periphery. Only in normoxia and varying oxygen conditions, some cells in the centre of the tumour do continue to divide (only visible after 7 days of growth). This may be due to the changes in the tumour microenvironment with the increased cell death at the centre. As the cells die, more nutrients will be available to quiescent cells to enable them to renter proliferating phase. Moreover, spatial changes due to the shrinkage of dead cells can influence the availability of nutrients at the centre. This might show a mechanism by which the tumour can grow back after a period of harsh conditions, for example quiescence
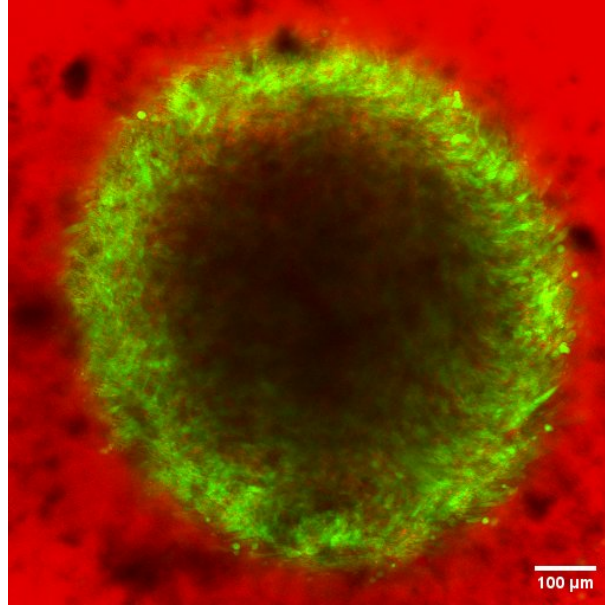
11

Figure 5: Picture of a spheroid grown for 30 days. Cells were marked using the fluorescent proteins Green FLuorescent Protein (GFP) and Sulforhodamine B (SRB). Living cells are colored in green, dying cells appear in red. The centre of the tumour is composed of hypoxic and dead cells, both do not emit fluorescence.

can be a mechanism to avoid drugs effect for the tumour cell [29]. Necrotic core has been observed in biological experiments run in the lab (figure 5).

It seems that varying the concentration of oxygen from normoxia to hypoxia, and reversing this process, every 6 hours doesn't affect the diameter of the tumour at the end of the simulation. However, a ring of necrotic cells in the swelling phase appears thicker than in other conditions.

Results in figure 6 show acid production according to the extracellular oxygen concentration. Red line y-axis intercept is equal to 0.02085 mmol/L (2% O_2), which corresponds to the threshold of hypoxia in physiological conditions. It is the level at which HIF has a half-maximal response as well [10]. Cells above this level are considered to be in normoxia while the rest of the cells are in hypoxia. Levels of extracellular oxygen fall below the hypoxia threshold after 2 days of growth in normoxic conditions (a necrotic core in the centre of the tumour has already formed). Due to poor oxygen concentration, cells with higher glycolytic activity appear and reach a H^+ production rate of almost 5×10^{-4} mmol/L/min. The maximum glycolytic activity of cells falls at 7 days of growth because of reduced glucose availability. When tumour growth is started in hypoxic conditions, high glycolytic activity is present after only one day of growth. In those conditions, the way the cell produces its energy is influenced only by glucose concentrations (similar to the result shown in figure 3). Therefore, hypoxic conditions directly select cells with high glycolytic activity.

The fact that, in the model, hypoxia may select cells with high glycolytic activity is supported by the levels of LDH/PDH genes presented in figure 7. In normoxia, cells have a level of LDH and PDH of 1 for both, it can be associated to an oxidative state. In hypoxia, LDH level reaches 3.0 and PDH level falls to 0.25, it can be associated to a glycolytic state. At the beginning of the simulation in normoxic conditions,
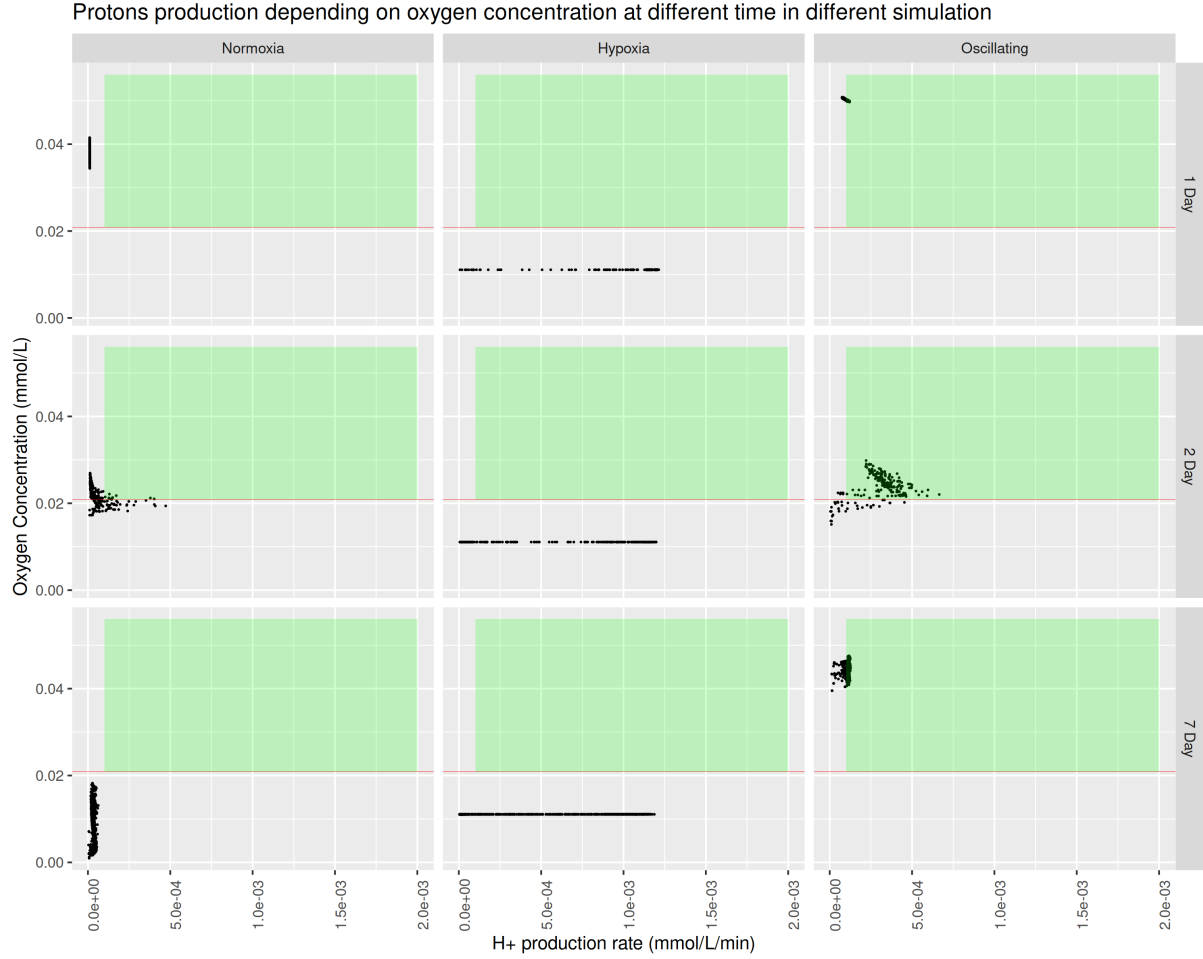
Figure 6: Acid production rate following oxygen extracellular concentrations at different times in different conditions. The red line indicates the hypoxia threshold. In oscillating conditions, oxygen concentration is slowly decreased from normoxia to hypoxia during 6h, then oxygen is increased to normoxia at the same rate. This process is repeated until the end of the simulation. Only living cells are represented on the graph. The green rectangle represents the region corresponding to a Warburg effect.
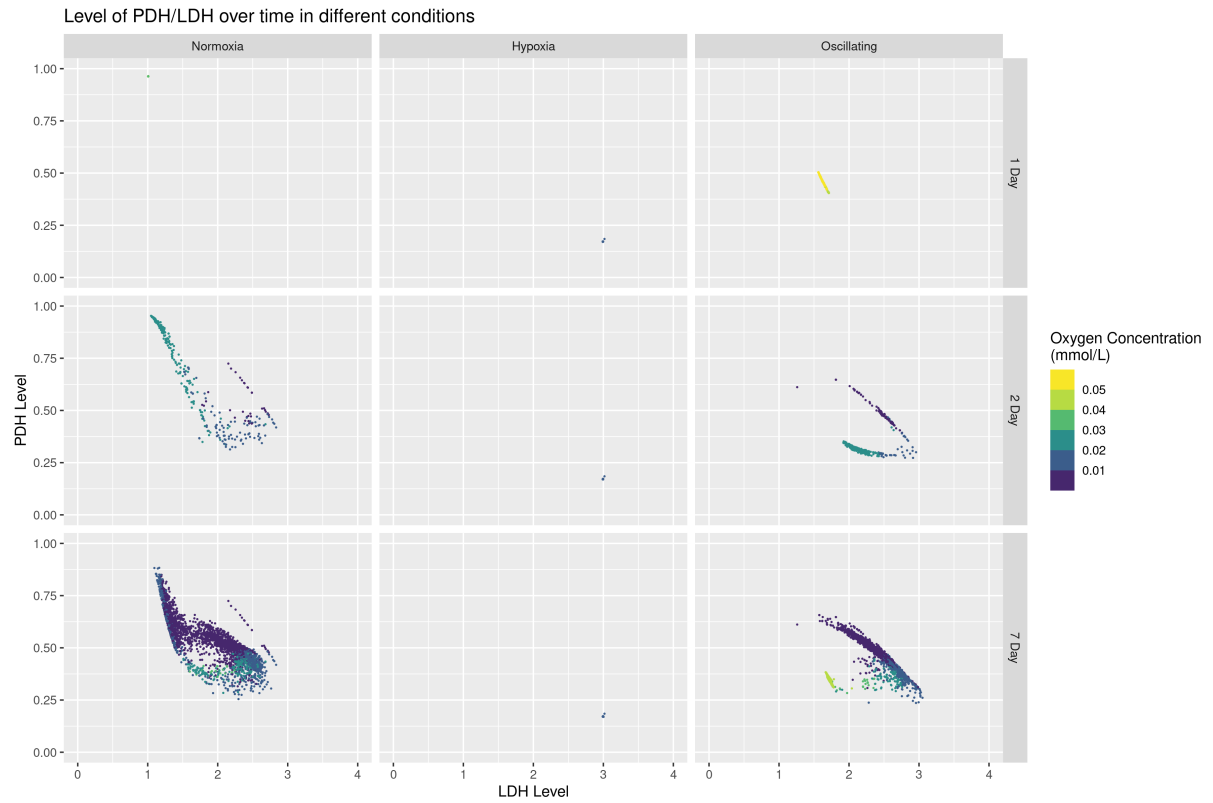
Figure 7: Plot of level of PDH against the level of LDH coloured by the extracellular oxygen concentration. The graph shows the results at different times for different conditions. In oscillating conditions, oxygen concentration is slowly decreased from normoxia to hypoxia during 6h, then oxygen is increased to normoxia at the same rate. This process is repeated until the end of the simulation. Only living cell are represented on the graph.

cells have 1:1 LDH/PDH levels. As the simulation goes, oxygen becomes less available. Thus LDH level increases while PDH level decreases. The result in normoxic conditions shows that cells migrate from an oxidative to a glycolytic state as oxygen concentration decreases. Cells around 2:0.5 LDH/PDH levels have a hybrid state where they rely on both nutrients to produce ATP. Again hypoxia selects for cells with high levels of LDH and low levels of PDH, suppressing the possibility for the cell to adopt a hybrid state.

Interestingly, extracellular oxygen concentration after 7 days is higher when oxygen varies between normoxia and hypoxia every 6 hours than in constant normoxia. Since cells are put in hypoxia several times a day, they rely more on glycolysis and consume less oxygen. Cells with higher glycolytic activity $(2.5 \times 10^{-4}\mathrm{mmol/L/min})$ even above the threshold of hypoxia appear at 2 days. It suggests that the Warburg Effect can be caused by environmental conditions with rapid variations. Combined with figure 7, genetic levels seems to indicate that cells cannot enter a complete oxidative state and are trapped either in a hybrid or a glycolytic state.

Influence of the intrinsic genetic properties of the cell

In figure 8, tumour growth is initiated in normoxia. Extracellular oxygen concentrations only vary due to cells consumption and reduced diffusion in the tumour. Only genetics regulations have been modified between each simulation to assess the impact of different genetic deregulations (mutations or epigenetic alterations) on tumour growth and cell metabolism. Results are similar to normoxic conditions with no genetic deregulations (figure 4). When reducing inhibition of PDH by PDK, tumour radius at 7 days of growth is lower than in normoxia and higher than in hypoxia with no mutation.

Figure 9 shows that cells start to become hypoxic after day 1, reaching a majority by day 2. After 7 days with a reduced HIF degradation rate by oxygen, extracellular oxygen goes back to normoxic levels yet cells have a higher acid production rate that corresponds to a Warburg effect. In this case, we suppose that cells slowly drain oxygen levels in the environment to a point where hypoxia is reached. Due to poor oxygen conditions, cells adapt their metabolism to enter a glycolytic state that they keep even if the oxygen supply goes back above 2 %O_2. Together with the result in figure 10, this might be caused by a delay in the response from returning to normal conditions since HIF regulation by O_2 is affected. While some cells have levels of LDH greater than 2 and PDH lower than 0.50 (hybrid to glycolytic state), some have a ratio of LDH/PDH almost equal to 1:1. This suggests that the Warburg Effect isn't irreversible with a reduced HIF degradation rate by oxygen alone.

As expected, reducing the increase in LDH levels due to HIF response doesn't induce a high acidification rate in normoxia but affects the maximum acid production rate and level of LDH. Instead of inducing a glycolytic phenotype, it seems to repress it.

Reducing the inhibiting power of PDK on PDH allows the cell to keep a higher PDH level, a key enzyme for oxygen consumption and oxidative state in the model. Cells exhibit an acid production rate similar to those in hypoxic conditions after 2 and 7 days, compared to other genetics deregulation. While in normoxia with no genetic deregulation cells seem to fluctuate around the threshold of hypoxia, here they are all below this level. Since PDH isn't effectively regulated by HIF, the cell tends to stay in an
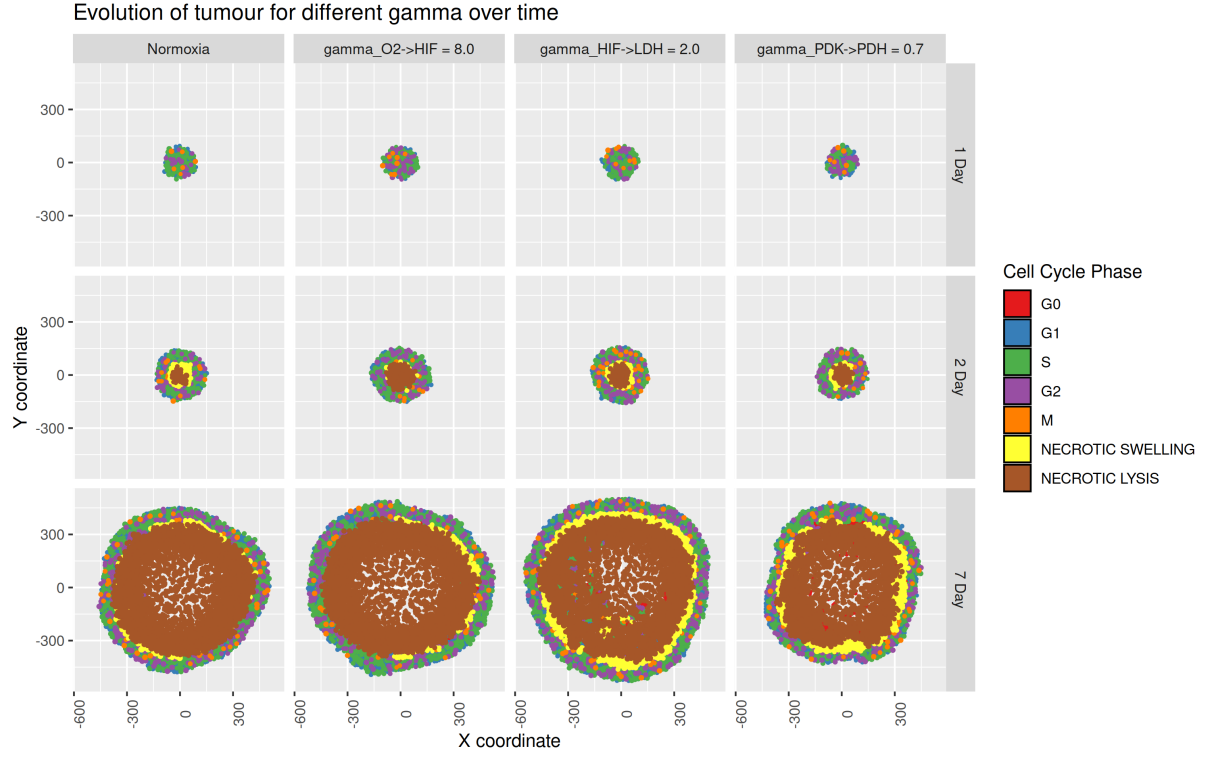
Figure 8: Evolution of tumour growth at different time with different genetic perturbations: reduced oxygen induced degradation of HIF ($\gamma O_2 \rightarrow HIF = 8.0$), lower use of glycolysis in hypoxic conditions ($\gamma HIF \rightarrow LDH = 2.0$) and lower effect of hypoxia on oxygen consumption ($\gamma PDK \rightarrow PDH = 0.7$). The normoxia conditions represent the growth with base parameters or no genetic deregulation ($\gamma O_2 \rightarrow HIF = 10.0$, $\gamma HIF \rightarrow LDH = 3.61$, $\gamma PDK \rightarrow PDH = 0.14$). New values have been selected following a qualitative exploration of the parameters effect on the model at the cell scale. Tumour growth was initiated in normoxia in all the simulations.
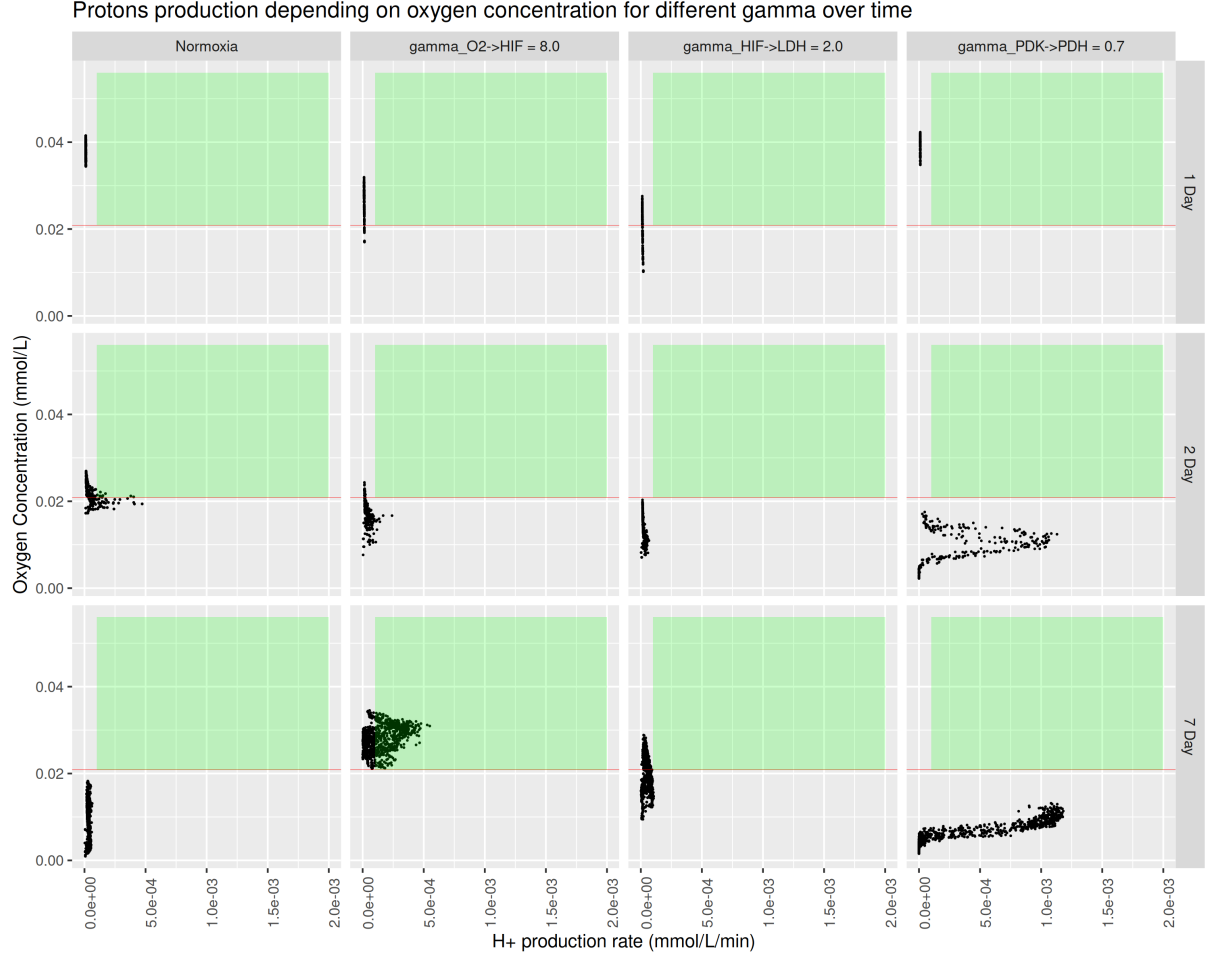
Figure 9: Acid production rate following oxygen extracellular concentrations at different times with different genetic perturbations. The red line indicates the hypoxia threshold. Only living cell are represented on the graph. Three genetics pertubations have been selected: reduced oxygen induced degradation of HIF ($\gamma O_2 \rightarrow HIF = 8.0$), lower use of glycolysis in hypoxic conditions ($\gamma HIF \rightarrow LDH = 2.0$) and lower effect of hypoxia on oxygen consumption ($\gamma PDK \rightarrow PDH = 0.7$). Tumour growth was initiated in normoxia. The green rectangle represents the region corresponding to a Warburg effect.
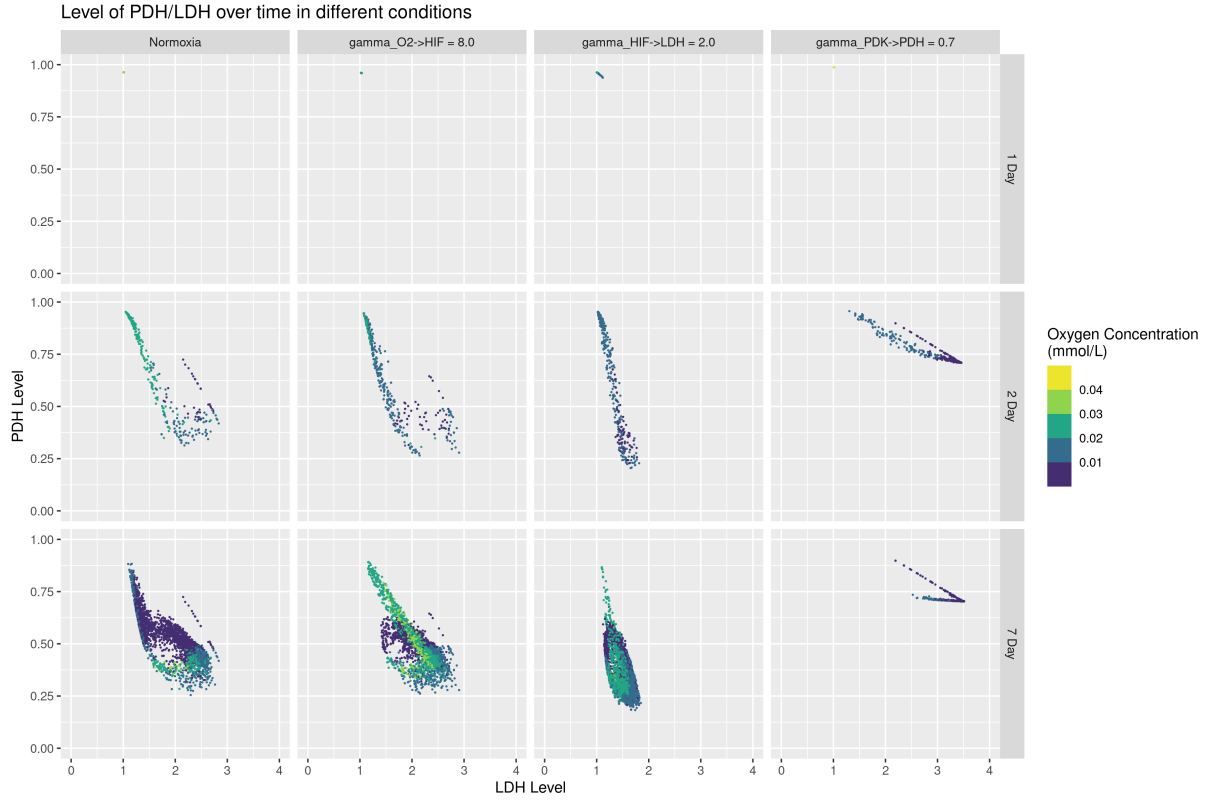
Figure 10: Plot of level of PDH against the level of LDH coloured by the extracellular oxygen concentration. The graph shows the results at different times with three different genetic perturbations: reduced oxygen induced degradation of HIF ($\gamma O_2 \rightarrow HIF = 8.0$), lower use of glycolysis in hypoxic conditions ($\gamma HIF \rightarrow LDH = 2.0$) and lower effect of hypoxia on oxygen consumption ($\gamma PDK \rightarrow PDH = 0.7$). Tumour growth was initiated in normoxia.

oxidative state and rely less on glycolysis. We can suppose that cells consume oxygen even when the level fall, creating further harder conditions. Results also show that adaptation to hypoxia is delayed and the cell only adopts a glycolytic state at oxygen conditions near-pathological hypoxia. PDH levels don't fall far below 0.75 even after 7 days of growth compared to others conditions, indicating that cells can only adopt an oxidative or hybrid state.

Discussion

In this paper, we formulated a mathematical model to study the impact of HIF on LDH and PDH, key enzymes of glycolysis and TCA cycle and thus investigating its role in cellular metabolism. Since its discovery, HIF has been actively studied by the scientific community. There are several modelling approaches to study the effects of HIF [25, 21, 18, 23] and here, we investigate its role using a multi-agent model, considering a heterogeneous environment that changes over time. Furthermore, the model is used to investigate the impact of genes on metabolism and the effect of different environmental conditions and different genetic deregulations (such as mutations or epigenetic alterations) can have on the Warburg Effect, an overproduction of acidity due to and increased glycolysis even in normoxia. Over-production of lactate can also be caused by reduced use of pyruvate in the mitochondria, remaining pyruvate is then turned into lactate.

Using the level of LDH and PDH genes as markers, we can define three different metabolic states like [21, 23]: oxidative, glycolytic and hybrid. The oxidative state corresponds to a high level of PDH and a low level of LDH, and inversely in a glycolytic state. The hybrid state then corresponds to medium levels of both enzymes, 2:0.5 for LDH and PDH respectively. As expected, normoxia strongly selects for the first state while hypoxia selects for the second one. The hybrid state is observed as the oxygen levels change over time due to tumour growth. Thus it appears that the cell adopts this state when adapting to changing oxygen conditions or when oxygen levels vary between normoxia and hypxia several times during tumour growth (oscillating conditions in the model).

We observed some differences between our model and the model in a recent paper from Li *et al* [21]: (1) they identified a normal state with a level of LDH at 1 and a level of PDH at 0.1, (2) their oxidative and glycolytic states have different levels of genes than those present in our model. This difference in the result can be explained by the fact that we only include a small fraction of their gene regulation network in our model, to only account for the effect caused by HIF.

We have simulated tumour growth when oxygen supply doesn't vary over time, hence differences in extracellular oxygen level can only be caused by cell consumption or reduced diffusion owing to higher cell density. We found that when there are rapid changes in oxygen supply to the tumour, cells with higher glycolytic rates above the threshold of hypoxia appear. It shows that varying microenvironmental conditions are sufficient to induce a Warburg phenotype for the cell. The results are inline with the findings by Damaghi *et al* [9]. However, the model doesn't include sudden genetic mutation which can be caused by harsh conditions. Therefore, in our case cell would not be trapped into a Warburg phenotype and this state can be reversed to a normal state if the cell is given enough time in favourable conditions.

Lactate secretion, which decreases the extracellular pH, depends on glucose consumption. A study from Casciari *et al* [30] has shown that a lower extracellular pH decreases dramatically glucose consumption, the Warburg effect could also be inhibited by low pH (6.95). We may suppose that after difficult conditions genes may be over-expressed or inhibited which will force the cell to adopt a Warburg phenotype.

The importance of HIF degradation in normoxia is further highlighted by the model results. We were also able to induce a Warburg effect by reducing the degradation rate of HIF by oxygen-dependent enzymes. Our results show that this effect only appears after a first period of hypoxia. It suggests that HIF accumulation forces the cell to adopt a glycolytic state and prevent it from returning to an oxidative state in normoxia. HIF inhibition therapy would prevent the appearance of Warburg cell type in cancer. PI3K and mTOR, two genes that increase HIF level independently of the level of oxygen [11, 14, 13], are studied as potential targets in anti-cancer therapy due to their altered expression in cancer and their role in signalling pathways affecting many biological functions [31, 32], possibly causing HIF overexpression. AMPK enzyme is known to interact with HIF [23] and inhibits its expression, some evidence link this gene to anti-tumour activity [33]. Those interactions could be added in further modelling work to study their impact on the Warburg effect as they may be important players interacting with HIF.

It has been shown that extracellular pH can (1) influence the cell metabolism (reduce glucose consumption, increase the cells doubling time) [30], (2) affect the ability of tumour cells to form metastasis, invade other tissue or migrate [34] and (3) could be a mechanism of invasion [35]. Currently, therapy targeting extracellular pH in the tumour are under development. Moreover, pH also affects the efficiency of different drugs such as temozolomide [36]. Reducing the increase in LDH level by the cell response to hypoxia lowered the rate of acid production in our simulation. Inhibitor of LDH could be used in combination with pH targeting therapy to improve treatment outcomes.

Reducing the down-regulation of PDH by HIF in the model forces the cell to rely as much as possible on oxygen to produce its energy. Herein, changes in metabolism toward glycolytic activity requires lower levels of oxygen. A study has shown that inhibition of HIF resulted in reduced lactate production, increase in oxygen consumption and radiotherapy sensitivity [7]. Whether increasing oxygen consumption by PDH upregulation would result in better outcomes in therapy in the model remains to be studied.

Conclusion

The main interest of the model is its ability to qualitatively describe HIF expression in tumour development over time with oxygen diffusion that depends on both cell consumption and cell density in the tumour to obtain a more realistic diffusion. Results of the model show that varying oxygen levels and reduced HIF degradation can cause increased glycolytic activity in normal oxygen levels. In the model, the emergence of the Warburg effect is preceded by a first period of hypoxia before returning to normoxic concentrations. This suggests that adaptation to environmental conditions is the primary phenomenon to understanding the Warburg effect. Interfering with the genetic activity of HIF or its effect on LDH and PDH may be used in therapy to induce specific behaviour in the cell.

Acknowledgements

Conflicts of Interest

The authors declare no conflict of interest.

References

[1] R. A. Bender. "Glycolysis". In: *Brenner's Encyclopedia of Genetics: Second Edition* 2 (2013), pp. 346–349. DOI: 10.1016/B978-0-12-374984-0.00659-8.

[2] Thomas C. King. "Cell Injury, Cellular Responses to Injury, and Cell Death". In: *Elsevier's Integrated Pathology* (2007), pp. 1–20. DOI: 10.1016/b978-0-323-04328-1.50007-3.

[3] F K Zimmermann. "Glycolysis in Saccharomyces cerevisiae". In: *Encyclopedia of Genetics* (2001), pp. 885–888. DOI: 10.1006/rwgn.2001.0570.

[4] Blanco, Antonio and Gustavo Blanco. "Medical Biochemistry . Academic Press, 2018." In: (2017), pp. 283–323. DOI: 10.1016/B978-0-12-803550-4/00014-8.

[5] Otto Warburg, Franz Wind, and Erwin Negelein. "The metabolism of tumors in the body". In: *Journal of General Physiology* 8.6 (1927), pp. 519–530. ISSN: 15407748. DOI: 10.1085/jgp.8.6.519. URL: https://www.ncbi.nlm.nih.gov/pmc/articles/PMC2140820/.

[6] Pierre Jacquet and Angélique Stéphanou. "Metabolic Reprogramming, Questioning, and Implications for Cancer". In: *Biology 2021, Vol. 10, Page 129* 10.2 (Feb. 2021), p. 129. ISSN: 20797737. DOI: 10.3390/BIOLOGY10020129. URL: https://www.mdpi.com/2079-7737/10/2/129/htm%20https://www.mdpi.com/2079-7737/10/2/129.

[7] Eric Leung et al. "Metabolic targeting of HIF-dependent glycolysis reduces lactate, increases oxygen consumption and enhances response to high-dose single-fraction radiotherapy in hypoxic solid tumors". In: *BMC Cancer* 17.1 (Dec. 2017), p. 418. ISSN: 1471-2407. DOI: 10.1186/s12885-017-3402-6. URL: https://bmccancer.biomedcentral.com/articles/10.1186/s12885-017-3402-6.

[8] Ian F. Robey et al. "Hypoxia-inducible factor-1α and the glycolytic phenotype in tumors". In: *Neoplasia* 7.4 (2005), pp. 324–330. ISSN: 15228002. DOI: 10.1593/neo.04430. URL: /pmc/articles/PMC1501147/?report=abstract%20https://www.ncbi.nlm.nih.gov/pmc/articles/PMC1501147/.

[9]   Mehdi Damaghi et al. "The Harsh Microenvironment in Early Breast Cancer Selects for a Warburg Phenotype". In: *bioRxiv* (Apr. 2020), p. 2020.04.07.029975. DOI: 10.1101/2020.04.07.029975. URL: https://doi.org/10.1101/2020.04.07.029975.

[10]   S. R. McKeown. *Defining normoxia, physoxia and hypoxia in tumours - Implications for treatment response.* Mar. 2014. DOI: 10.1259/bjr.20130676. URL: /pmc/articles/PMC4064601/%20/pmc/articles/PMC4064601/?report=abstract%20https://www.ncbi.nlm.nih.gov/pmc/articles/PMC4064601/.

[11]   Georgina N. Masoud and Wei Li. "HIF-1α pathway: Role, regulation and intervention for cancer therapy". In: *Acta Pharmaceutica Sinica B* 5.5 (2015). ISSN: 22113843. DOI: 10.1016/j.apsb.2015.05.007. URL: https://www.sciencedirect.com/science/article/pii/S2211383515000817?pes=vor.

[12]   J. Xu et al. "Epigenetic regulation of HIF-1α in renal cancer cells involves HIF-1α/2α binding to a reverse hypoxia-response element". In: *Oncogene* 31.8 (2012). ISSN: 09509232. DOI: 10.1038/onc.2011.305. URL: https://pubmed.ncbi.nlm.nih.gov/21841824/%20https://www.nature.com/articles/onc2011305.

[13]   Ji-Won Lee et al. "Hypoxia-inducible factor (HIF -1)alpha : its protein stability and biological function s". In: *Experimental and Molecular Medicine* 36.1 (2004), pp. 1–12. DOI: 10.1038/emm.2004.1. URL: https://www.nature.com/articles/emm20041.

[14]   Yoshihiro Hayashi et al. "Hypoxia/pseudohypoxia-mediated activation of hypoxia-inducible factor-1α in cancer". In: *Cancer Science* 110.5 (May 2019), pp. 1510–1517. ISSN: 1347-9032. DOI: 10.1111/cas.13990. URL: https://onlinelibrary.wiley.com/doi/abs/10.1111/cas.13990.

[15]   Roger McLendon et al. "Comprehensive genomic characterization defines human glioblastoma genes and core pathways". In: *Nature* 455.7216 (2008), pp. 1061–1068. ISSN: 00280836. DOI: 10.1038/nature07385. URL: https://www.nature.com/articles/nature07385.

[16]   Lucija Slemc and Tanja Kunej. "Transcription factor HIF1A: downstream targets, associated pathways, polymorphic hypoxia response element (HRE) sites, and initiative for standardization of reporting in scientific literature". In: *Tumor Biology* 37.11 (2016). ISSN: 14230380. DOI: 10.1007/s13277-016-5331-4. URL: https://link.springer.com/article/10.1007/s13277-016-5331-4.

[17]   Nobuhito Goda, Sara J. Dozier, and Randall S. Johnson. *HIF-1 in cell cycle regulation, apoptosis, and tumor progression.* July 2003. DOI: 10.1089/152308603768295212. URL: https://www.liebertpub.com/doi/abs/10.1089/152308603768295212.

[18]   B. Bedessem and A. Stéphanou. "A mathematical model of HiF-1α-mediated response to hypoxia on the G1/S transition". In: *Mathematical Biosciences* 248.1 (2014), pp. 31–39. ISSN: 00255564. DOI: 10.1016/j.mbs.2013.11.007. URL: http://dx.doi.org/10.1016/j.mbs.2013.11.007.

[19]   Shabnam Heydarzadeh et al. *Regulators of glucose uptake in thyroid cancer cell lines.* June 2020. DOI: 10.1186/s12964-020-00586-x. URL: https://doi.org/10.1186/s12964-020-00586-x.

[20] Alvaro Marin-Hernandez et al. "HIF-1alpha Modulates Energy Metabolism in Cancer Cells by Inducing Over-Expression of Specific Glycolytic Isoforms". In: *Mini-Reviews in Medicinal Chemistry* 9.9 (Aug. 2009), pp. 1084–1101. ISSN: 13895575. DOI: 10.2174/138955709788922610. URL: http://www.eurekaselect.com/openurl/content.php?genre=article&issn=1389-5575&volume=9&issue=9&spage=1084.

[21] Wenbo Li and Jin Wang. "Uncovering the Underlying Mechanisms of Cancer Metabolism through the Landscapes and Probability Flux Quantifications". In: *iScience* 23.4 (Apr. 2020), p. 101002. ISSN: 25890042. DOI: 10.1016/j.isci.2020.101002. URL: https://doi.org/10.1016/j.isci.2020.101002.

[22] Kieran Smallbone et al. "Metabolic changes during carcinogenesis: potential impact on invasiveness". In: *Journal of theoretical biology* 244.4 (Feb. 2007), pp. 703–713. ISSN: 0022-5193. DOI: 10.1016/J.JTBI.2006.09.010. URL: https://pubmed.ncbi.nlm.nih.gov/17055536/.

[23] Dongya Jia et al. "Elucidating cancer metabolic plasticity by coupling gene regulation with metabolic pathways". In: *Proceedings of the National Academy of Sciences of the United States of America* 116.9 (Feb. 2019), pp. 3909–3918. ISSN: 10916490. DOI: 10.1073/pnas.1816391116. URL: https://pubmed.ncbi.nlm.nih.gov/30733294/.

[24] Rupert Courtnay et al. "Cancer metabolism and the Warburg effect: the role of HIF-1 and PI3K". In: *Molecular biology reports* 42.4 (2015), pp. 841–851. ISSN: 15734978. DOI: 10.1007/s11033-015-3858-x.

[25] Mark Robertson-Tessi et al. "Impact of Metabolic Heterogeneity on Tumor Growth, Invasion, and Treatment Outcomes". In: *Cancer Research* 75.8 (Apr. 2015), pp. 1567–1579. ISSN: 0008-5472. DOI: 10.1158/0008-5472.CAN-14-1428. URL: http://cancerres.aacrjournals.org/lookup/doi/10.1158/0008-5472.CAN-14-1428.

[26] Jerry J. Zimmerman, Amélie von Saint André-von Arnim, and Jerry McLaughlin. *Cellular Respiration*. Fourth Edi. Elsevier, 2011, pp. 1058–1072. ISBN: 9780323073073. DOI: 10.1016/B978-0-323-07307-3.10074-6. URL: http://dx.doi.org/10.1016/B978-0-323-07307-3.10074-6.

[27] Ahmadreza Ghaffarizadeh et al. "PhysiCell: An open source physics-based cell simulator for 3-D multicellular systems". In: *PLOS Computational Biology* 14.2 (Feb. 2018), e1005991. ISSN: 1553-7358. DOI: 10.1371/JOURNAL.PCBI.1005991. URL: https://journals.plos.org/ploscompbiol/article?id=10.1371/journal.pcbi.1005991.

[28] Geoffrey M Cooper. "The Eukaryotic Cell Cycle". In: (2000). URL: https://www.ncbi.nlm.nih.gov/books/NBK9876/.

[29] Tomás Alarcón and Henrik Jeldtoft Jensen. "Quiescence: A mechanism for escaping the effects of drug on cell populations". In: *Journal of the Royal Society Interface* 8.54 (2011), pp. 99–106. ISSN: 17425662. DOI: 10.1098/rsif.2010.0130. arXiv: 1002.4579.

[30] Joseph J. Casciari, Stratis V. Sotirchos, and Robert M. Sutherland. "Variations in tumor cell growth rates and metabolism with oxygen concentration, glucose concentration, and extracellular pH". In: *Journal of Cellular Physiology* 151.2 (1992), pp. 386–394. ISSN: 10974652. DOI: 10.1002/jcp.1041510220.

[31] Jing Yang et al. *Targeting PI3K in cancer: Mechanisms and advances in clinical trials.* 2019. DOI: 10.1186/s12943-019-0954-x.

[32] Tian Tian, Xiaoyi Li, and Jinhua Zhang. *mTOR signaling in cancer and mtor inhibitors in solid tumor targeting therapy.* 2019. DOI: 10.3390/ijms20030755.

[33] Weidong Li et al. *Targeting AMPK for cancer prevention and treatment.* 2015. DOI: 10.18632/oncotarget.3629.

[34] S. D. Webb, J. A. Sherratt, and R. G. Fish. "Mathematical Modelling of Tumor Acidity: Regulation of Intracellular pH". In: *Journal of Theoretical Biology* 196.2 (Jan. 1999), pp. 237–250. ISSN: 0022-5193. DOI: 10.1006/JTBI.1998.0836. URL: https://doi.org/10.1006/jtbi.1998.0836.

[35] Kieran Smallbone, Robert A. Gatenby, and Philip K. Maini. "Mathematical modelling of tumour acidity". In: *Journal of Theoretical Biology* 255.1 (2008), pp. 106–112. ISSN: 00225193. DOI: 10.1016/j.jtbi.2008.08.002.

[36] Angélique Stéphanou and Annabelle Ballesta. "pH as a potential therapeutic target to improve temozolomide antitumor efficacy : A mechanistic modeling study". In: *Pharmacology Research and Perspectives* 7.1 (Feb. 2019). ISSN: 20521707. DOI: 10.1002/PRP2.454.